Chem

CellPress

Article

Covalent Organic Frameworks Linked by Amine Bonding for Concerted Electrochemical Reduction of CO_2

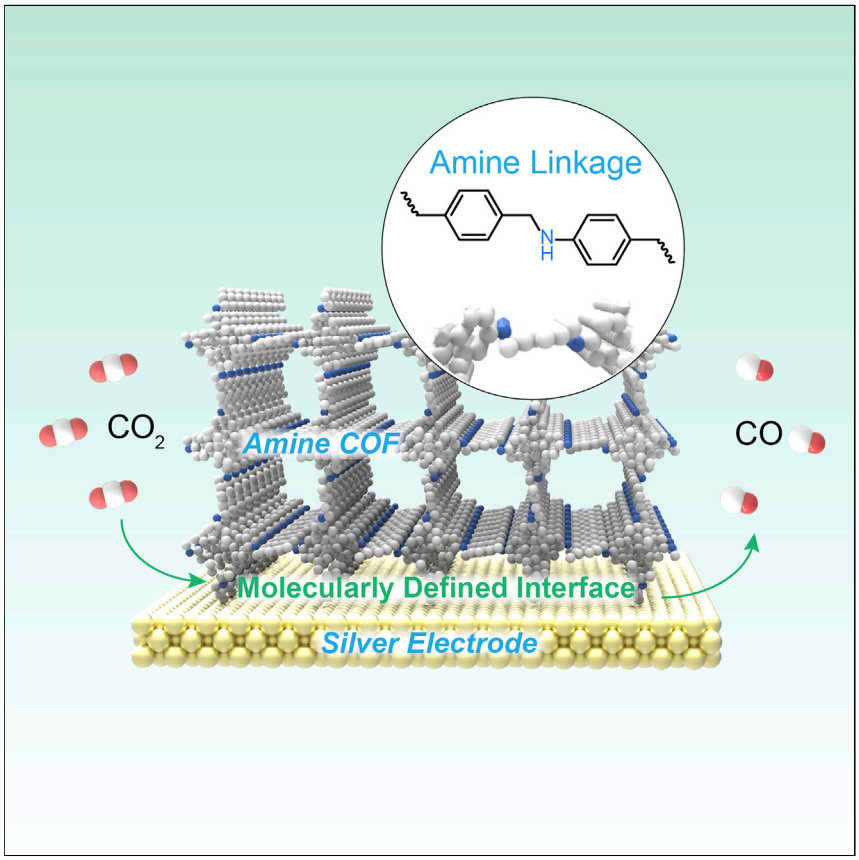

Amine-linked covalent organic frameworks (COFs) were synthesized by the reduction of parent imine-linked COFs by crystal-to-crystal transformation. The excellent chemical stability of these COFs in combination with the presence of a large amount of amine functional groups led to a robust and molecularly defined interface at the silver metal surface as an electrode for the electrochemical reduction of CO_2. The concerted operation of COF and the metal surface resulted in high conversion efficiency and excellent selectivity against the reduction of water.

Haoyu Liu, Jun Chu, Zhenglei Yin, Xin Cai, Lin Zhuang, Hexiang Deng

hdeng@whu.edu.cn

HIGHLIGHTS

Synthesis of amine-linked COFs in both 2D and 3D forms

Stability in both strong acid and base

Construction of molecularly defined interface

Electrochemical reduction of CO_2 with high efficiency and selectivity

Liu et al., Chem 4, 1–14
July 12, 2018
https://doi.org/10.1016/j.chempr.2018.05.003

Please cite this article in press as: Liu et al., Covalent Organic Frameworks Linked by Amine Bonding for Concerted Electrochemical Reduction of CO_2, Chem (2018), https://doi.org/10.1016/j.chempr.2018.05.003

Chem

CellPress

Article

Covalent Organic Frameworks Linked by Amine Bonding for Concerted Electrochemical Reduction of CO_2

Haoyu Liu,[1] Jun Chu,[2] Zhenglei Yin,[1] Xin Cai,[2] Lin Zhuang,[1,2] and Hexiang Deng[1,2,3,*]

SUMMARY

Covalent organic frameworks (COFs) with amine linkage in both three and two dimensions, COF-300-AR and COF-366-M-AR, were synthesized by direct reduction of their corresponding COFs with imine linkage, COF-300 and COF-366-M, respectively. The quantitative reduction was confirmed by Fourier transform infrared and cross-polarization magic angle spinning NMR (both ^{13}C and ^{15}N) spectroscopy. These amine COFs were highly crystalline and exhibited excellent chemical stability in strong acids and bases. The abundant amino groups in the COF-300-AR backbone facilitated the electrochemical reduction of CO_2 on silver electrodes in a concerted manner and led to selective generation of CO. Specifically, CO conversion efficiency was raised from 13% to 53% at −0.70 V and from 43% to 80% at −0.85 V (versus a reversible hydrogen electrode) in comparison with that of a bare silver electrode. The porosity of COFs favored molecular diffusion to the electrode surface, and the amine functional groups close to the electrode surface promoted CO_2 conversion efficiency by forming carbamate intermediates.

INTRODUCTION

Covalent organic frameworks (COFs) are widely used for the storage, separation, and conversion of gases, because they provide molecularly defined pores to interact with guest molecules.[1–7] Although highly desirable for catalytic applications, chemically stable COFs were hard to synthesize because of the dilemma between the strength of the linkage and the microscopic reversibility required for the crystallization process.[8–12] Efforts to form strong covalent bonds in COFs via *de novo* synthesis usually resulted in amorphous phase rather than crystalline structure.[13,14] Recently, Waller et al. reported a method for addressing this challenge, whereby the entire framework structure of a two-dimensional (2D) COF made from labile linkages (imines) is directly converted by oxidation reactions to highly stable linkages (amides) without altering the original structural topology or order.[15] In the present article, we show that amine-based COFs, heretofore unknown, can be produced by the application of reduction reactions directly on the imine-linked frameworks. We demonstrated this reduction for both 2D and three-dimensional (3D) COFs, COF-366-M and COF-300,[16–18] respectively, to generate their corresponding secondary amine frameworks, COF-366-M-AR (2D COF) and COF-300-AR (3D COF), where AR stands for "after reduction," and M = Co, Cu, and Zn. The crystallinity and underlying topology of both 2D and 3D frameworks are fully retained throughout the conversion process. The newly formed amine linkage provides exceptional chemical and thermal stability for these COFs far beyond their imine parent structures. Their crystallinity is unaltered after immersion in a 6 M HCl and

The Bigger Picture

By extending covalent bonds to two-dimensional (2D) and three-dimensional (3D) frameworks, the emergence of covalent organic frameworks (COFs) represents a new and exciting branch in porous and crystalline materials. Currently, the discovery of new linkages and improvement of chemical stability are the two most pressing challenges for the development of COFs. We report the synthesis of an amine-linked COFs in both 2D and 3D forms. These COFs exhibited excellent stability in strong acid and base. Furthermore, by depositing COF-300-AR on a flat silver electrode, we were able to construct a molecularly defined interface for electrochemical reduction of CO_2 to CO with high efficiency and selectivity. Spectroscopic studies revealed that the concerted behavior between COFs and the silver electrode at their interface was responsible for the promoted performance. This molecularly defined interface approach improves the selectivity of the electrochemical reaction without sacrificing the overall efficiency.

6 M NaOH solution for more than 12 hr. The power of this solid-state conversion is that it obviates the trial-and-error method intrinsic to *de novo* synthesis of COFs and can be used to synthesize chemically robust COFs with new linkages that are not easily obtained otherwise.

Furthermore, we applied one of the amine COFs, COF-300-AR, to the electrochemical reduction of CO_2 in aqueous media, where both the chemical stability of the framework and the amine functionality in the backbone play critical roles. COF-300-AR particles were deposited on a silver electrode with a flat surface to form a molecularly defined interface for the catalytic reaction. Compared with a bare silver electrode, this interface provided excellent selectivity of the CO_2 reduction reaction (CO_2RR) against the H_2 evolution reaction (HER). Such improvement in selectivity originates from the concerted environment endowed by the amine COFs and the metal surface. The secondary amine linkages in the COF backbone provide chemisorptive sites to selectively capture CO_2 molecules by forming carbamates, as shown by ^{13}C solid-state nuclear magnetic resonance, and the silver surface activates the carbamates and provides sufficient electrons for their reduction to CO.

Previous efforts to improve CO_2RR selectivity involved either the use of a molecular catalytic center, where the electron-transfer efficiency was largely affected by the conductivity of such material, or the use of small inactive molecules to modify the surface of the metal electrode, where the accessibility of CO_2 was limited by their coverage.[19–24] In this study, we constructed an ordered porous environment on the surface of a metal electrode to form a molecularly defined interface, where CO_2 diffusion was favored and excellent CO_2RR selectivity was provided without sacrificing the current of the original metal electrode.

RESULTS AND DISCUSSION

Reduction of 2D and 3D COFs and Characterizations

Amine linkages have been extensively used in polymer chemistry, and amine macromolecules have been widely used as surfactants and in biomedical applications.[25,26] Theoretically, amine linkages can be obtained by the reduction of imine linkages, which are common in the formation of COFs. Although both oxidation and reduction have been used extensively in organic molecules, such quantitative conversions in extended solids are rare because of the limit in diffusion of the reactants and the flexibility of the targeting functional groups.[27–29] In order to identify a suitable condition to achieve solid-state conversion of imine to amine linkages in COFs, at first we used a commercially available compound, benzylidene aniline, as a model. Among various reductive conditions tested in this study, we identified that the best method involved the use of $NaBH_4$, by which quantitative conversion of benzylidene aniline to benzyl aniline was achieved (Figure 1A). This was confirmed by the appearance of new peaks at 1,603 and 1,266 cm^{-1} from benzyl aniline and the disappearance of the 1,626 cm^{-1} peak from benzylidene aniline in the Fourier-transform infrared (FTIR) spectrum of the product (Figure 1C). The formation of benzyl aniline was also verified by ^1H nuclear magnetic resonance (NMR) (Figure S17).

Applying this optimized reduction condition, two classic imine COFs covering both 2D and 3D topologies were successfully converted to amine COFs. The 3D COF, COF-300, was obtained by linking tetra-(4-anilyl) methane and terephthalaldehyde (Figure 1B), and the 2D COF, COF-366-M (M = Co, Zn, and Cu), was obtained by linking [5,10,15,20-tetrakis(4-aminophenyl) porphinato]-M and

[1]UC Berkeley-Wuhan University Joint Innovative Center, Institute for Advanced Studies, Wuhan University, Luojiashan, Wuhan 430072, China

[2]College of Chemistry and Molecular Sciences, Wuhan University, Luojiashan, Wuhan 430072, China

[3]Lead Contact

*Correspondence: hdeng@whu.edu.cn

https://doi.org/10.1016/j.chempr.2018.05.003

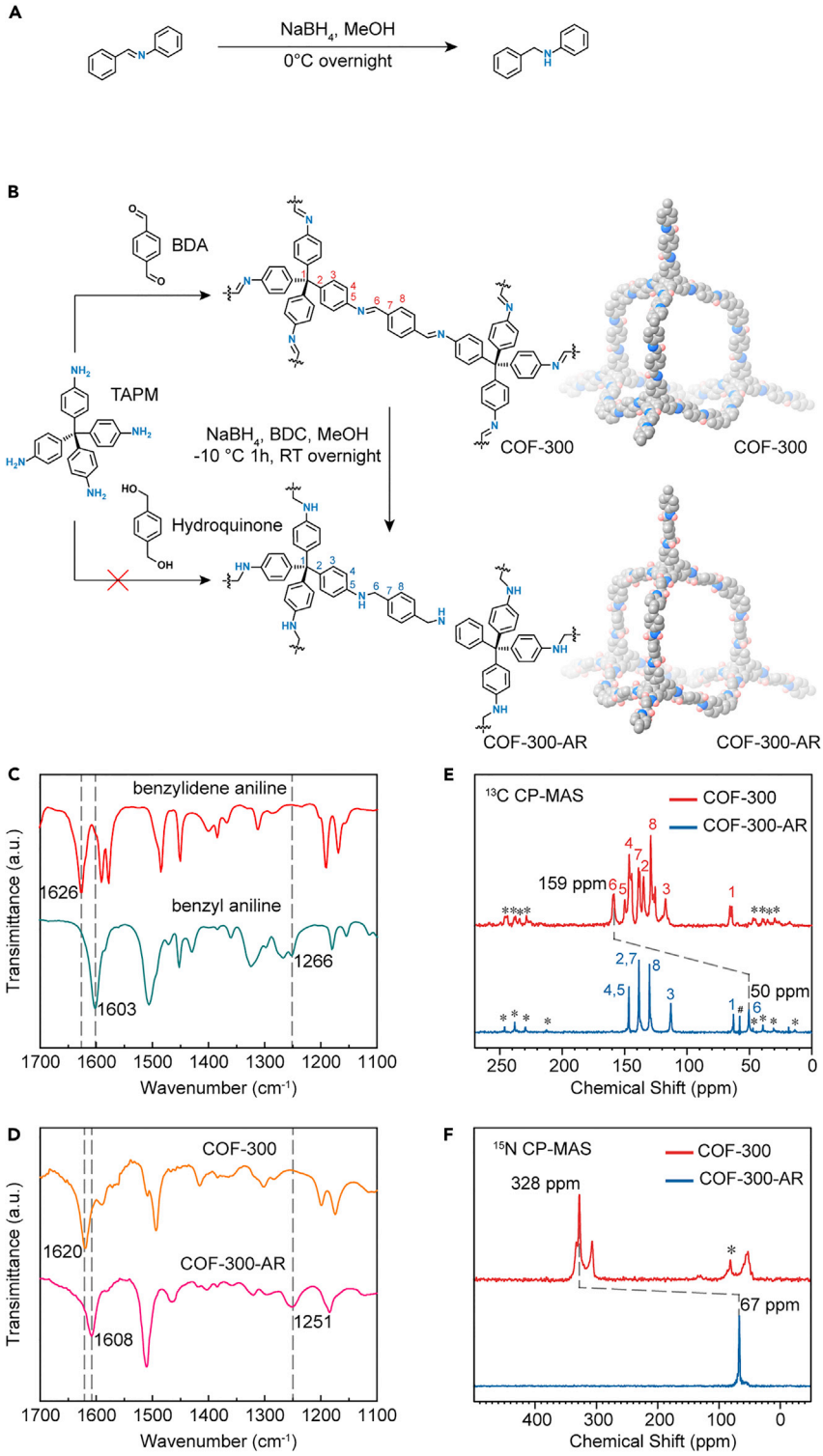

Figure 1. Model Reaction and Reduction of COF-300 with Imine to Form COF-300-AR with Amine Linkage

(A) Scheme for model reaction.

(B) Scheme for COF-300 reduction. BDA, benzene-1,4-dicarboxaldehyde; TAPM, terta(4-aminophenyl)methane. In the space-filling diagrams, carbon and nitrogen atoms are

Please cite this article in press as: Liu et al., Covalent Organic Frameworks Linked by Amine Bonding for Concerted Electrochemical Reduction of CO_2, Chem (2018), https://doi.org/10.1016/j.chempr.2018.05.003

Figure 1. *Continued*
represented as gray and blue spheres, respectively. Only the hydrogen atoms on the imine and amine linkage are shown (in pink) for clarity.
(C) FTIR spectra of the model compound before and after reduction.
(D) FTIR spectra of COF-300 before and after reduction.
(E and F) ^{13}C (E) and ^{15}N (F) CP-MAS NMR spectra of COF-300 before and after reduction. ^{15}N-enriched samples were used in the ^{15}N CP-MAS NMR experiment. *, sideband; #, signal for carbon in ethanol.

terephthalaldehyde (Figure 2A). The successful conversion of the reduction reaction was confirmed by FTIR spectroscopy (Figure 1D). Similar to that of the molecular conversion, the new peaks at 1,251 cm^{-1} and 1,608 cm^{-1} represented C–N vibration stretch and C–N–H bending stretch in the secondary amine linkage. The disappearance of the 1,620 cm^{-1} peak, representing the C=N vibration stretch of imine in the parent COF-300 structure, demonstrated the complete conversion of this reaction. Similar phenomena were observed in FTIR spectra of COF-366-M and COF-366-M-AR (Figures 2B, S3, and S4). In addition, the quantitative conversion of imine to amine linkages was verified by both ^{13}C and ^{15}N cross-polarization magic angle spinning (CP/MAS) NMR spectroscopy (Figures 1E and 1F). After reduction, the imine carbon peak belonging to COF-300 at 159 ppm disappeared completely in the ^{13}C CP-MAS NMR spectrum, and a new peak at 50 ppm emerged, indicating the formation of amine linkages (Figure 1E). A trace amount of ethanol was added to COF-300-AR to increase the flexibility of the framework backbone; thus, sharper peaks were observed in the CP-MAS NMR experiment (Figure 1E). In ^{15}N CP-MAS NMR experiments, both the COF-300 and COF-300-AR samples were ^{15}N enriched with the use of tetra-(4-anilyl) methane linkers labeled with ^{15}N for the synthesis. The disappearance of the imine nitrogen peak at 307 ppm and the emergence of an amine nitrogen peak at 53 ppm also demonstrated the successful conversion from imine to amine linkage in the COF structure (Figure 1F). We noticed that there were multiple peaks in addition to the major imine peak in the parent COF-300 structure, which might originate from the unreacted linkers trapped in the framework.[14] In contrast, only one sharp peak was observed in the ^{15}N CP-MAS NMR spectrum of COF-300-AR, representing the uniform chemical environments of amine linkages in the COF backbone. It is likely that the reduction process purged the impurities from the COF structure.

Unlike the amorphous product usually observed in previous studies to form amine bonds in extended structure, the crystallinity and the underlying topology of the parent COF were well preserved in this solid-state chemical conversion. The reduced COF samples were examined by powder X-ray diffraction (PXRD) using a synchrotron radiation source (wavelength, λ = 1.23980 Å). Sharp peaks were clearly observed in their PXRD patterns, indicating high crystallinity. PXRD patterns of both COF-300-AR and COF-366-Cu-AR samples are in good agreement with those of the original COFs tested under the same conditions (Figures 3A, 3B, and S11). Pawley refinement was applied against the experimental PXRD patterns to obtain the lattice parameters of the original and reduced COF-300 crystals. The same tetragonal *I41/a* space group was identified in both crystals with a slight change in the lattice parameters from 27.2269 to 27.0632 Å in *a* and from 11.5153 to 11.5339 Å in *c* for COF-300 and COF-300-AR, respectively. This variation can be attributed to the change in the hybridization of carbon and nitrogen atoms, from sp^2 in the imine linkage in COF-300 to sp^3 in the amine linkage in COF-300-AR. Similar observations can also be found in the reduction of COF-366 (Figure S10B). Although the number of peaks was limited in the PXRD pattern of COF-366-Cu-AR, it was clear that its crystallinity and the underlying topology were unaltered.

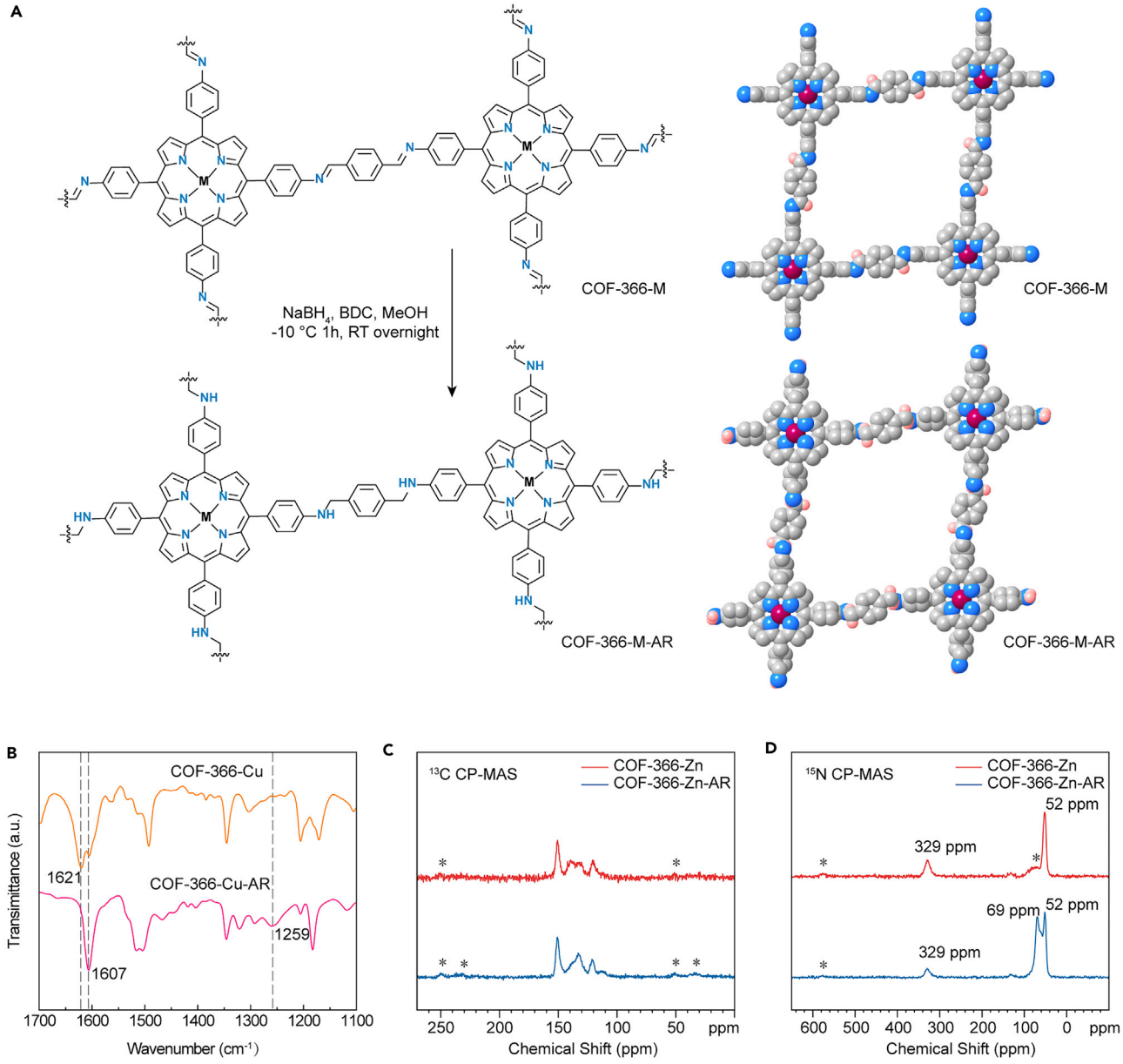

Figure 2. Reduction of COF-366-M Series with Imine Linkages to COF-366-M-AR Series with Amine Linkages

(A) Scheme for the reduction of COF-366-M (M = Co, Cu, or Zn). In the space-filling diagrams, carbon and nitrogen atoms are represented as gray and blue spheres, respectively. Only the hydrogen atoms on the imine and amine linkage are shown (in pink) for clarity.

(B) FTIR spectra of COF-366-Cu before and after reduction.

(C and D) ^{13}C (C) and ^{15}N (D) CP-MAS NMR spectra of COF-366-Zn and COF-366-Zn-AR. ^{15}N enriched samples were used in the ^{15}N CP-MAS NMR experiment. *, sideband.

In order to confirm the preservation of the underlying pore structure of COF-300-AR, inclusion experiments were conducted to introduce small organic molecules into the COF pores. Here, we diffused tetraphenylethylene (TPE), a fluorescent molecule, into the pores of COF-300-AR, and the inclusion of this fluorescent molecule was characterized by laser scanning confocal microscopy. Blue fluorescence of TPE was observed across the entire COF crystal, indicating the successful inclusion of TPE (largest dimension of 11.7 Å) into the pores of COF-300-AR (Figures S30 and S31).

Please cite this article in press as: Liu et al., Covalent Organic Frameworks Linked by Amine Bonding for Concerted Electrochemical Reduction of CO_2, Chem (2018), https://doi.org/10.1016/j.chempr.2018.05.003

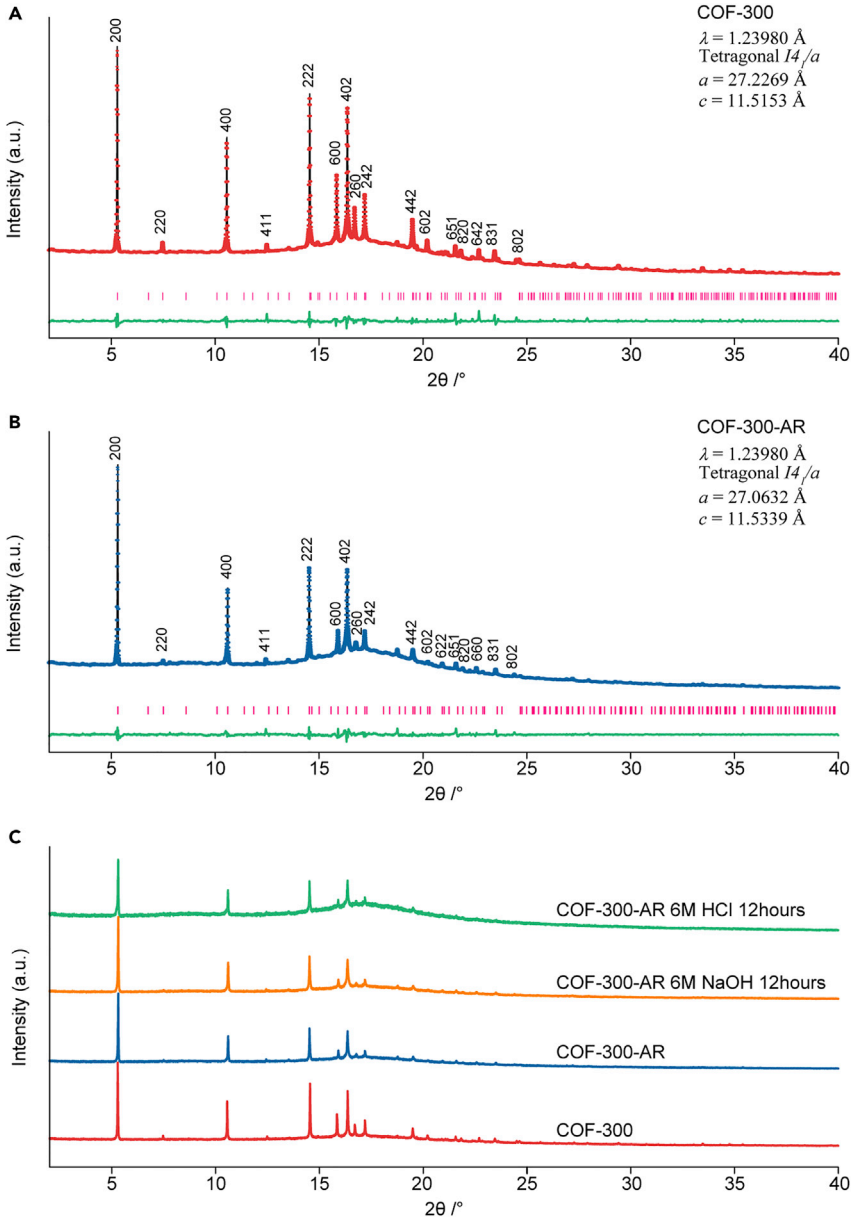

Figure 3. Crystallinity and Chemical Stability of the Amine COFs

(A and B) PXRD patterns of COF-300 before (A) and after (B) reduction. Pawley refinement was performed against the diffraction patterns and the results showed that the crystallinity was well maintained after conversion of imine linkages to amine linkages.

(C) Unaltered PXRD patterns of COF-300-AR demonstrated excellent stability in both strong acid and base. Wavelength of the X-ray source is 1.23980 Å.

Stability Test for Reduced COFs

The advantage of the amine linkages is their overwhelming chemical stability compared with that of imine linkages. In order to demonstrate the chemical stability of the amine COFs, we immersed COF-300-AR samples in extremely acidic and basic aqueous solutions: 6 M HCl (pH < 0) and 6 M NaOH (pH > 14), respectively. After immersion for 12 hr, PXRD patterns of COF samples were collected with a synchrotron X-ray source (wavelength, λ = 1.23980 Å). Sharp peaks identical to those

Please cite this article in press as: Liu et al., Covalent Organic Frameworks Linked by Amine Bonding for Concerted Electrochemical Reduction of CO_2, Chem (2018), https://doi.org/10.1016/j.chempr.2018.05.003

of the pre-immersion samples were observed, demonstrating unaltered crystallinity of the amine COFs after immersion (Figure 3C). In contrast, the imine COF, COF-300, was dissolved completely in 6 M HCl under the same conditions. In the immersion test in 6 M NaOH, the crystallinity of COF-300 was partially preserved (Figure S11). Upper clear solutions were also collected for ^{1}H NMR study after the immersion tests in acid. Multiple peaks present in the solution of the COF-300 test, which can be assigned as fingerprint peaks for two molecular building blocks of this COF (tetraphenylmethane and benzene-1,4-dicarboxaldehyde). This further indicated the decomposition of imine COF under acid conditions. However, no observable peaks except for the solvent peaks were found in that of the COF-300-AR test. It is clear that the chemical stability of COFs was drastically improved as the imine linkages were converted to amine linkages (Figure S18).

Electrochemical Reduction of CO_2 Performed by Concerted Electrode

One of the key challenges for electrochemical CO_2 reduction using metal electrodes is the lack of selectivity toward the desirable product, although the kinetics of total conversion are rather high. Intrinsically, this originates from the flat band structure of the metal and the lower potential of the competing hydrogen evolution. In contrast, molecular complex provides discrete frontier orbitals that can interact with CO_2 molecules in specific orientations, thus providing excellent selectivity. When these complexes were used in electrochemical catalysis, however, the overall reaction kinetics was limited because of the electron-transfer barrier between the electrode and the catalytic center in the molecule. In this study, we designed a molecularly defined interface by combining the catalytic surface of the Ag electrode with the ordered porous amino environment of COFs, which is attractive for CO_2 molecules (Figure 4A). Ideally, CO_2 conversion will take place between the metal surface and the orderly arranged amino functional groups dangling above; thus, CO_2 molecules can directly accept electrons from the metal surface rather than through the COF framework (Figure 4B). In this way, the reaction kinetics was well preserved, and the selectivity was guaranteed by the molecularly defined environment. The interface was constructed by a thin layer of COF-300-AR deposited homogeneously on a flat silver electrode, as confirmed by scanning electron microscopy (SEM) and energy dispersive X-ray spectrometer (EDX) mapping (Figures 4C–4F). The silver surface was rather smooth, as visualized in the Ag Lα EDX image, and the thickness of COF-300-AR layer was 15 μm, as revealed in the C Kα1 EDX image.

This COF-Ag interface was subjected to CO_2 electrochemical reduction tests. The onset potential representing the initiation of CO_2 reduction was −0.50 V versus a reversible hydrogen electrode (RHE) for COF-decorated silver electrode, which was similar to that of the bare silver electrode (Figure S19). Compared with COF on the bare silver electrode, COF on the silver electrode exhibited an increased faradic efficiency (FE) of CO from 13% to 53% and 43% to 80% under the potential of −0.70 and −0.85 V versus RHE, respectively (Figures 5C and 5D); on the other hand, the HER was obviously suppressed from 80% to 22% and 60% to 9% under −0.70 and −0.85 V versus RHE, respectively. Two control experiments were performed under identical conditions. No obvious improvement in CO_2 conversion selectivity was observed on the silver electrode using only Nafion binder (Figures 5C and 5D), whereas almost no CO_2 conversion took place on the glassy carbon electrode decorated with COF-300-AR. In addition, COF-300 was used as another control for a electrochemical CO_2 conversion study, where the total current decreased obviously (Figure S26), and there was no improvement in either catalytic efficiency or selectivity (Figures S27 and S28). It is clear that the drastic increase in

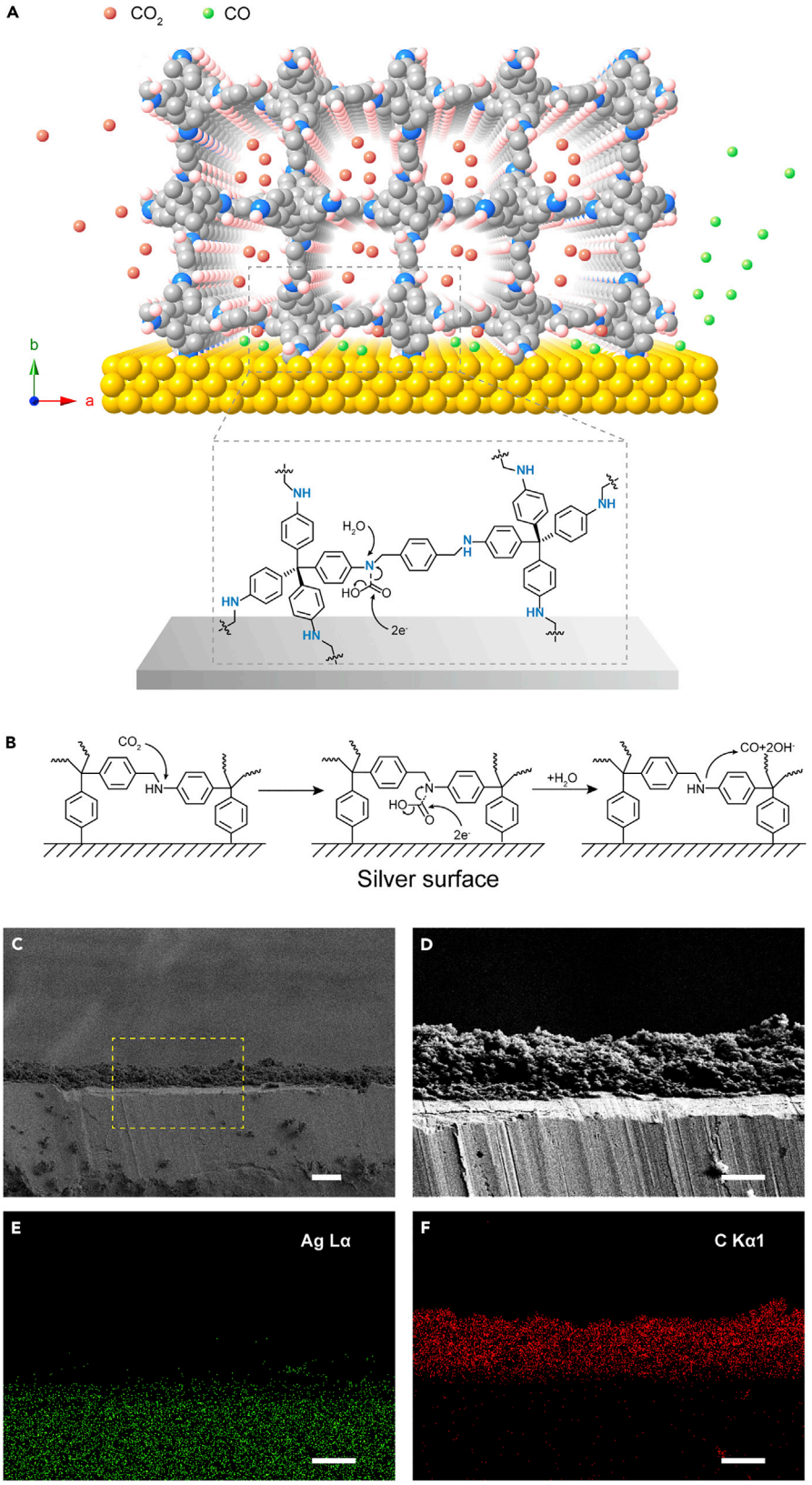
A
CO2
CO
b
a
NH
HN
H2O
HO
O
2e-
B
CO2
+H2O
CO+2OH-
Silver surface
C
D
E
Ag Lα
F
C Kα1

Please cite this article in press as: Liu et al., Covalent Organic Frameworks Linked by Amine Bonding for Concerted Electrochemical Reduction of CO_2, Chem (2018), https://doi.org/10.1016/j.chempr.2018.05.003

Figure 4. Molecularly Defined Interface Created by COF-300-AR on a Flat Silver Electrode

(A) Illustration of the molecularly defined interface.

(B) Scheme of the mechanism of concerted CO_2 reduction taking place at the interface between COFs and the silver electrode through the critical carbamate formation. Electrons directly transferred to the CO_2 molecules that were activated by the amine functional groups in the COF structure.

(C–F) SEM images and elemental mapping of the molecularly defined interface between COF and the silver electrode; the SEM image was taken at 5 keV, and energy dispersive spectroscopy mapping was taken at 10 keV Ag Lα (E; green) and C Kα (F; red). Scale bars: 20 μm (C) and 10 μm (D–F).

CO_2RR activity on the silver electrode decorated with COF-300-AR originates from the concerted effect between COFs and the surface of the silver electrode.

Study on Interaction and Mechanism Proposal

In order to glimpse into the mechanism of selective CO_2 conversion on the concerted electrode, CO_2 adsorption was tested on a COF-300-AR sample, and ^{13}C-labeled CO_2 was introduced in a CP/MAS NMR experiment for this COF. The affinity between COF-300-AR and CO_2 was demonstrated by CO_2 isotherms collected at both 273 K and 298 K (Figure 5A). The hysteresis between the desorption and adsorption curves indicated strong interaction between the amine framework and CO_2 molecules. In order to identify the type of this interaction between CO_2 and COF-300-AR, ^{13}C CP/MAS NMR spectroscopy was applied on COF samples before and after absorbing CO_2 (Figure 5B). A strong peak at 162.3 ppm emerged in the spectrum of COF samples after exposure to ^{13}C-labeled CO_2 at 1 bar, corresponding to the formation of carbamate. This demonstrated the presence of chemisorption between COF-300-AR and CO_2 molecules. In addition, high-power decoupling ^{13}C NMR spectra were performed on the same sample without spinning. Compared with the dominating carbamate peak at 162.3 ppm, a tiny peak at 125.3 ppm was observed, indicating physically absorbed CO_2 molecules also existed in the pores of COF-300-AR (Figure 5B).[30] The dominating chemisorption was also confirmed by FTIR spectroscopy of COF-300-AR exposed to CO_2, where two new peaks at 1,629 and 1,650 cm^{-1} appeared, representing the formation of carbamate (Figure S14). These results demonstrated that the formation of carbamate is the key transition state before CO_2 molecules receive electrons from the Ag electrode to be reduced to CO (Figure 4B). Here, we propose a mechanism for the CO_2 conversion on the concerted electrode. First, CO_2 molecules were attracted by the amine framework and then interacted with the amine functional groups hanging above the electrode to form carbamates. Second, the formation of carbamate further promoted the conversion of CO_2 at the molecularly defined Ag surface, and an excessive amount of electrons can be transferred without going through the COF backbone. Third, facilitated by water molecules, the carbamates were reduced to CO molecules and OH^- anions; thus, the amino functional groups in the COF structure were regenerated to close the catalytic cycle (Figure 4B). The OH^- anions generated in the aqueous solution diffused to the counter electrode through an anionic membrane to generate O_2.

Conclusion

In this study, we synthesized highly crystalline amine COFs with both 3D and 2D topologies through solid-state conversion from their corresponding imine COFs. The amine linkage provided excellent chemical stability for the framework, and the underlying topology was preserved. In principle, this conversion can be generally applied to any imine COFs. The amine COFs were applied in electrochemical reduction of CO_2 in this study, representing a promising application for porous frameworks with amine functional groups. Carbamate was identified to be the key intermediate for an efficient CO_2 reduction process. The high FE and drastically improved selectivity of CO_2RR over HER originated from the molecularly defined

Please cite this article in press as: Liu et al., Covalent Organic Frameworks Linked by Amine Bonding for Concerted Electrochemical Reduction of CO_2, Chem (2018), https://doi.org/10.1016/j.chempr.2018.05.003

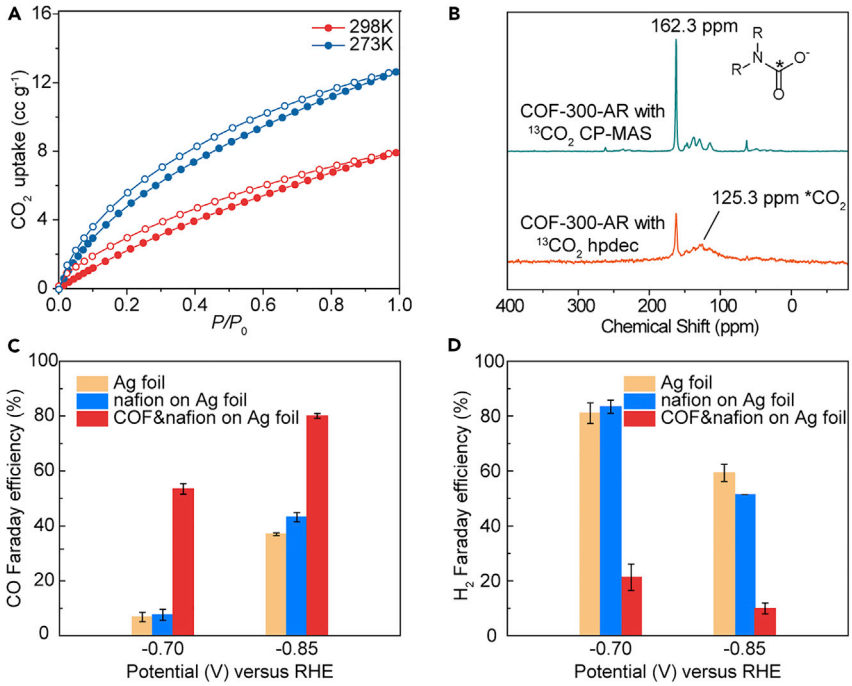

Figure 5. Investigation of Interactions between COF-300-AR and CO_2, and Electrochemical Performance of CO_2 Reduction

(A) CO_2 adsorption isotherms of COF-300-AR at 273 and 298 K.

(B) ^{13}C CP-MAS NMR showing the formation of carbamate intermediate during CO_2 reduction process.

(C and D) Faradic efficiency for CO (C) and H_2 (D) production on the concerted electrode of COF-300-AR and Ag at various potentials. Bare silver foil and Nafion solution were used as controls. Error bars represent the FE from two independent measurements.

interface constructed by amine COF and the silver electrode in a concerted manner. The construction of a concerted electrode represents a promising direction for accessing high efficiency and selectivity in electrochemical catalytic reactions, especially for energy storage and conversion.

EXPERIMENTAL PROCEDURES

Reduction Procedure

A general procedure is presented below. The equivalences are calculated on the basis of the number of imine functionalities in the COF.

General notes: all reagents must be of high purity. The imine COFs used in the reduction conversion were prepared by sequential solvent exchange with 1,4-dioxine and acetone by Soxhlet extractor, followed by supercritical carbon dioxide activation.

COF-300-AR: *p*-phthalic acid (57.6 mg, 0.347 mmol, 1 equiv) was added to the suspension of COF-300 samples (50 mg, 0.347 mmol by imine) in 25 mL of MeOH. The mixture was stirred at −15°C for 5 min before $NaBH_4$ (0.5 g, 13.22 mmol, 38 equiv) was added in small portions over a period of 10 min. After stirring at −15°C for 1 hr, the mixture was stirred at room temperature for another 10 hr. A light-yellow solid could be collected either by centrifugation or filtration. The reduced COF,

Please cite this article in press as: Liu et al., Covalent Organic Frameworks Linked by Amine Bonding for Concerted Electrochemical Reduction of CO_2, Chem (2018), https://doi.org/10.1016/j.chempr.2018.05.003

COF-300-AR, samples were then washed with water three times, extracted with ethanol for 24 hr (with a Soxhlet extractor), and then dried under dynamic vacuum at room temperature. Elemental analysis (EA) of activated COF-300-AR samples is as follows: calcd C 84.25%, H 6.16%, N 9.59%; found C 81.93%, H 5.86%, N 9.44%.

COF-366-M-AR: the synthesis of COF-366-MAR was carried out according to a protocol similar to that used for COF-300-AR. In the synthesis, the COF-300 sample was replaced with COF-366-Co (50 mg, 0.054 mmol by imine), COF-366-Cu (50 mg, 0.054 mmol by imine), and COF-366-Zn (50 mg, 0.054 mmol by imine), and the rest of the synthetic procedure was the same as for COF-300-AR. EA of the activated COF-366-Co-AR sample is as follows: calcd C 77.00%, H 4.70%, N 11.98%; found C 76.62%, H 4.70%, N 12.37%. EA of COF-366-Cu-AR is as follows: calcd C 76.78%, H 4.51%, N 11.94%; found C 72.84%, H 4.70%, N 11.02%. EA of COF-366-Zn-AR is as follows: calcd C 76.63%, H 4.50%, N 11.92%; found C 76.08%, H 4.52%, N 9.81%.

Material Characterizations

PXRD data were recorded on both synchrotron and laboratory-based X-ray sources. The laboratory-based PXRD patterns were collected on a Rigaku Smartlab 9 kW diffractometer in reflection mode operated at 45 kV, 200 mA for Cu Kα (λ = 1.5406 Å) with a scan speed of 1°/min and a step of 0.01° in 2θ at ambient temperature and pressure. The synchrotron-based PXRD patterns were performed in transmission mode at beamline BL14B1 in the Shanghai Synchrotron Radiation Facility (SSRF) with a wavelength of 1.2398 Å. Samples were held in a sealed capillary with a drop of ethanol inside. Thermogravimetric analysis (TGA) was performed on a TA Instruments Q-500 series thermal gravimetric analyzer with samples held in platinum pans in a continuous nitrogen or air flow atmosphere. The heating rate was 10°C/min throughout the TGA experiments. Elemental microanalyses were performed in the Center of Material Research and Analysis at Wuhan University of Technology with an Elementar Vario EL cube elemental analyzer. FTIR spectra were recorded on a Nicolet NEXUS670 IR spectroscope, and samples were tableted with KBr as support. Liquid-state NMR spectra were referenced with the chemical shift of solvent peaks.

Electrochemical Experiments

Preparation of Ag Electrode and COF-Ag Electrode

The Ag electrode was prepared by polishing Ag foil bought from Alfa Aesar and subsequent washing with deionized (DI) water and ethanol three times each. Ten milligrams of COF-300-AR was mixed with 40 μL of Nafion solution, 250 μL of ethanol, and 750 μL of DI water and then placed in an ultrasonic bath for 2 min. This mixture was dropped onto the Ag foil and dried with an infrared lamp to prepare it for testing. In the control experiment, 40 μL of Nafion solution, 250 μL of ethanol, and 750 μL of DI water were mixed and then dropped on another Ag foil under identical conditions.

Electrochemical Measurements

The electrochemical experiments were carried out in a homemade H-type electrolytic cell equipped with three electrodes with the working and counter electrode compartments separated by a Nafion membrane. The Ag foil served as the working electrode, and the counter electrode and the reference electrode were a sheet of carbon paper and the saturated calomel electrode (SCE), respectively. Electrochemical reduction of CO_2 was conducted in a CO_2-saturated atmosphere in the presence of 0.1 M $KHCO_3$ solution (pH 6.8), and the electrode potentials were converted to

the RHE reference scale with E (versus RHE) = E (versus SCE) + 0.2415 V + 0.0591 × pH, where 0.2415 V represents the standard potential of SCE with saturated KCl solution. The geometric area of the electrode was 0.50 cm^2.

Product Analysis

The major products of electrochemical reduction of CO_2 on the Ag electrode were gaseous products such as CO and H_2, in accordance with previous studies. The amount of H_2 and CO generated was quantified by online gas chromatography (GC) analysis (Shimadzu, GC-2010 plus) equipped with a ShinCarbon column (Restek) and a Barrier discharge ionization detector. In general, the cathodic compartment of the gas-tight H-type electrolytic cell was purged with CO_2 gas of high purity for at least 30 min before each measurement. In the CO_2 electrochemical conversion process, CO_2 was steadily bubbled to the cell at 5 sccm. The product gases went through the sampling loop and were analyzed by GC continuously during the potentiostatic electrolysis. The FE of the electrochemical reduction of CO_2 process was calculated as follows, by the corresponding peak area present in the chromatogram, which is calibrated by a certified standard gas.

$$FE = \frac{I_p}{I_t} \times 100\%,$$

$$I_p = \frac{V_p \times P \times nF}{RT},$$

$$V_p = \varphi_p \times V_t,$$

where φ_p is the volume fraction of the product derived from GC calibration, V_t is total gas flow rate, and R, T, P, n, and F represent the ideal gas constant, temperature, pressure, the number of electrons transferred, and faradic constant, respectively, plus the total current obtained from a potentiostat (CHI-720E). I_p is the current of product calculated from GC data; I_p is the total current.

SUPPLEMENTAL INFORMATION

Supplemental Information includes Supplemental Experimental Procedures, 31 figures, and 1 table and can be found with this article online at https://doi.org/10.1016/j.chempr.2018.05.003.

ACKNOWLEDGMENTS

This work was supported by the National Natural Science Foundation of China (21471118, 91545205, and 91622103), National Science Foundation of Jiangsu Province of China (ZXG201446 and BK20140410), National Key Basic Research Program of China (2014CB239203), Key Program of Hubei Provence (2015CFA126), and Innovation Team of Wuhan University (WHU) (2042017kf0232). We thank the Test Center and Core Research Facilities of WHU and Wuhan National Laboratory for Optoelectronics for providing technical support, beamline BL14B1 (SSRF) for providing the beam time and help during experiments, and Profs. F. Deng and J. Xu (National Center for Magnetic Resonance in Wuhan, Wuhan Institute of Physics and Mathematics, Chinese Academy of Sciences) for help with solid-state NMR experiments. Special thanks go to Prof. Y.-B. Zhang (School of Physical Science and Technology, ShanghaiTech University) for help with the crystal structure analysis, X. Wei (College of Chemistry and Molecular Science, WHU) for help with the FTIR test, and M. Tang (College of Life Science, WHU) for the fluorescence test. We also thank all group members' support and help in Deng's lab.

AUTHOR CONTRIBUTIONS

H.D. conceived the idea and led the project; H.L. and H.D. designed the COF reduction experiments; H.L. performed the reduction of COF-300; J.C. performed the reduction of the COF-366 series and, in a joint effort, characterized the structure and stability of the amine COFs; H.D. and L.Z. designed the electrochemical CO_2 reduction experiment; Z.Y., X.C., and H.L. performed the electrochemical experiments. H.L., X.C., and H.D. prepared the first version of the manuscript, and all authors contributed to the discussion of results and the final version.

DECLARATION OF INTERESTS

The authors declare no competing interests.

Received: December 11, 2017
Revised: January 21, 2018
Accepted: May 4, 2018
Published: June 14, 2018

REFERENCES AND NOTES

1. Côte, A.P., Benin, A.I., Ockwig, N.W., O'Keeffe, M., Matzger, A.J., and Yaghi, O.M. (2005). Porous, crystalline, covalent organic frameworks. Science *310*, 1166–1170.

2. Huang, N., Wang, P., and Jiang, D. (2016). Covalent organic frameworks: a materials platform for structural and functional designs. Nat. Rev. Mater. *1*, 16068.

3. DeBlase, C.R., and Dichtel, W.R. (2016). Moving beyond boron: the emergence of new linkage chemistries in covalent organic frameworks. Macromolecules *49*, 5297–5305.

4. Ding, S.Y., and Wang, W. (2013). Covalent organic frameworks (COFs): from design to applications. Chem. Soc. Rev. *42*, 548–568.

5. Ascherl, L., Sick, T., Margraf, J.T., Lapidus, S.H., Calik, M., Hettstedt, C., Karaghiosoff, K., Döblinger, M., Clark, T., Chapman, K.W., et al. (2016). Molecular docking sites designed for the generation of highly crystalline covalent organic frameworks. Nat. Chem. *8*, 310–316.

6. Das, S., Heasman, P., Ben, T., and Qiu, S. (2016). Porous organic materials: strategic design and structure–function correlation. Chem. Rev. *117*, 1515–1563.

7. Jin, Y., Hu, Y., and Zhang, W. (2017). Tessellated multiporous two-dimensional covalent organic frameworks. Nat. Rev. Chem. *1*, 0056.

8. Du, Y., Yang, H., Whiteley, J.M., Wan, S., Jin, Y., Lee, S.H., and Zhang, W. (2016). Ionic covalent organic frameworks with spiroborate linkage. Angew. Chem. Int. Ed. *55*, 1737–1741.

9. Kandambeth, S., Mallick, A., Lukose, B., Mane, M.V., Heine, T., and Banerjee, R. (2012). Construction of crystalline 2D covalent organic frameworks with remarkable chemical (acid/base) stability via a combined reversible and irreversible route. J. Am. Chem. Soc. *134*, 19524–19527.

10. Xu, H., Gao, J., and Jiang, D. (2015). Stable, crystalline, porous, covalent organic frameworks as a platform for chiral organocatalysts. Nat. Chem. *7*, 905–912.

11. Kandambeth, S., Shinde, D.B., Panda, M.K., Lukose, B., Heine, T., and Banerjee, R. (2013). Enhancement of chemical stability and crystallinity in porphyrin-containing covalent organic frameworks by intramolecular hydrogen bonds. Angew. Chem. Int. Ed. *125*, 13290–13294.

12. Li, L.H., Feng, X.L., Cui, X.H., Ma, Y.X., Ding, S.Y., and Wang, W. (2017). Salen-based covalent organic framework. J. Am. Chem. Soc. *139*, 6042–6045.

13. Smith, B.J., and Dichtel, W.R. (2014). Mechanistic studies of two-dimensional covalent organic frameworks rapidly polymerized from initially homogenous conditions. J. Am. Chem. Soc. *136*, 8783–8789.

14. Smith, B.J., Overholts, A.C., Hwang, N., and Dichtel, W.R. (2016). Insight into the crystallization of amorphous imine-linked polymer networks to 2D covalent organic frameworks. Chem. Commun. (Camb.) *52*, 3690–3693.

15. Waller, P.J., Lyle, S.J., Osborn Popp, T.M., Diercks, C.S., Reimer, J.A., and Yaghi, O.M. (2016). Chemical conversion of linkages in covalent organic frameworks. J. Am. Chem. Soc. *138*, 15519–15522.

16. Wan, S., Gándara, F., Asano, A., Furukawa, H., Saeki, A., Dey, S.K., Liao, L., Ambrogio, M.W., Botros, Y.Y., Duan, X., et al. (2011). Covalent organic frameworks with high charge carrier mobility. Chem. Mater. *23*, 4094–4097.

17. Lin, S., Diercks, C.S., Zhang, Y.B., Kornienko, N., Nichols, E.M., Zhao, Y.B., Paris, A.R., Kim, D., Yang, P.D., Yaghi, O.M., and Chang, C.J. (2015). Covalent organic frameworks comprising cobalt porphyrins for catalytic CO_2 reduction in water. Science *349*, 1208–1213.

18. Uribe-Romo, F.J., Hunt, J.R., Furukawa, H., Klöck, C., O'Keeffe, M., and Yaghi, O.M. (2009). A crystalline imine-linked 3-D porous covalent organic framework. J. Am. Chem. Soc. *131*, 4570–4571.

19. Chen, Y., Li, C.W., and Kanan, M.W. (2012). Aqueous CO_2 reduction at very low overpotential on oxide-derived Au nanoparticles. J. Am. Chem. Soc. *134*, 19969–19972.

20. Qiao, J., Liu, Y., Hong, F., and Zhang, J. (2014). A review of catalysts for the electroreduction of carbon dioxide to produce low-carbon fuels. Chem. Soc. Rev. *43*, 631–675.

21. Cook, T.R., Dogutan, D.K., Reece, S.Y., Surendranath, Y., Teets, T.S., and Nocera, D.G. (2010). Solar energy supply and storage for the legacy and nonlegacy worlds. Chem. Rev. *110*, 6474.

22. Trickett, C.A., Helal, A., Al-Maythalony, B.A., Yamani, Z.H., Cordova, K.E., and Yaghi, O.M. (2017). The chemistry of metal–organic frameworks for CO_2 capture, regeneration and conversion. Nat. Rev. Mater. *2*, 17045.

23. Zhu, D.D., Liu, J.L., and Qiao, S.Z. (2016). Recent advances in inorganic heterogeneous electrocatalysts for reduction of carbon dioxide. Adv. Mater. *28*, 3423–3452.

24. Kuhl, K.P., Hatsukade, T., Cave, E.R., Abram, D.N., Kibsgaard, J., and Jaramillo, T.F. (2014). Electrocatalytic conversion of carbon dioxide to methane and methanol on transition metal surfaces. J. Am. Chem. Soc. *136*, 14107–14113.

25. Pack, D.W., Hoffman, A.S., Pun, S., and Stayton, P.S. (2005). Design and development of polymers for gene delivery. Nat. Rev. Drug Discov. *4*, 581–593.

26. Holland, N.B., Qiu, Y., Ruegsegger, M., and Marchant, R.E. (1998). Biomimetic engineering of non-adhesive glycocalyx-like surfaces using oligosaccharide surfactant polymers. Nature *392*, 799–801.

27. Swamy, S.I., Bacsa, J., Jones, J.T., Stylianou, K.C., Steiner, A., Ritchie, L.K., Hasell, T., Gould, J.A., Laybourn, A., Khimyak, Y.Z., et al. (2010). A

metal–organic framework with a covalently prefabricated porous organic linker. J. Am. Chem. Soc. *132*, 12773–12775.

28. Liu, M., Little, M.A., Jelfs, K.E., Jones, J.T., Schmidtmann, M., Chong, S.Y., Hasell, T., and Cooper, A.I. (2014). Acid-and base-stable porous organic cages: shape persistence and pH stability via post-synthetic "tying" of a flexible amine cage. J. Am. Chem. Soc. *136*, 7583–7586.

29. Gui, B., Meng, X., Chen, Y., Tian, J., Liu, G., Shen, C., Zeller, M., Yuan, D., and Wang, C. (2015). Reversible tuning hydroquinone/quinone reaction in metal–organic framework: immobilized molecular switches in solid state. Chem. Mater. *27*, 6426–6431.

30. Li, D., Furukawa, H., Deng, H., Liu, C., Yaghi, O.M., and Eisenberg, D.S. (2014). Designed amyloid fibers as materials for selective carbon dioxide capture. Proc. Natl. Acad. Sci. USA *111*, 191–196.